Quantification and Compensation of Unintentional Analyte Aggregation in Electrospray Sampling

Mingdong Li[1,2], Suvajyoti Guha[1,2], Rebecca Zangmeister[2], Michael J. Tarlov[2], Michael R. Zachariah[1,2]

1. University of Maryland College Park, MD
2. National Institute of Standards and Technology, Gaithersburg, MD

Abstract

Electrospray (ES) sources are commonly used to introduce non-volatile materials (e.g. nanoparticles, proteins, etc.) in to the gas phase for characterization by mass spectrometry and ion mobility. Recent studies in our group using electrospray ion mobility to characterize protein aggregation in solution have raised the question as to whether the electrospray itself induces aggregation and thus corrupts the results. In this paper we develop a statistical model to determine the extent to which the ES process induces the formation of dimers and higher order aggregates. The model is validated through ES-differential mobility experiments using gold nanoparticles. The results show that the extent of droplet induced aggregation is quite severe, and that previously reported cut-off criterion are inadequate. We use the model in conjunction with experiment to show the true dimer concentration in a protein solution as a function of concentration. The model is extendable to any ES source-analytical system and to higher aggregation states.

1. Introduction

Protein aggregation is a major concern with nearly all protein therapeutics because of their potential for immunogenicity in patients. One of the tools we are investigating to measure protein aggregation involves using electrospray to generate vapor phase dispersed material. These vapor phase dispersed materials can then be analyzed by ion mobility methods named differential mobility analyzer (DMA) also known as gas-phase electrophoretic molecular analysis (GEMMA)[1-6] or mass spectrometry (MS)[7-10] methods. These techniques have the potential to characterize the distribution of oligomeric protein species in solution.

To accurately characterize protein oligomers in solution, the electrospray process shoud be thoroughly understood in order to correct for any potential bias originating from droplet formation. The mechanism of ES has been treated in great detail by Kebarle *et al.*[11] and Gaskell[12]. In ES, the application of a high voltage to a capillary will induce, due to columbic repulsion, small droplet formation. Those droplets undergo evaporation coupled with collisions, as well as fissions when reaching their Rayleigh limits. There are two major theories employed to explain the ES process to eventually produce gas phase analyte ions: charge residue model(CRM)[13] and ion evaporation model(IEM)[14,15]. In the IEM it is thought that the strong E-field at the drop surface results in ion-emission at a critical drop radius. CRM suggests that droplets undergo a series of fissions to a final drop size where subsequent solvent evaporation leaves behind the residue analyte (e.g. protein, particle, virus, etc). In this study we will not concern ourselves as to the

correctness of these mechanisms, as we will by-pass the nature of the ES-process by directly measuring the final droplet size distribution.

As mentioned, one of the potential uses of ES-DMA or ES-MS is to study oligomerization in solution. For this application one must consider whether the measured oligomer distribution reflects the actual distribution in the sample, or if the observed oligomers are an artifact of the ES process. For example, one potential concern is where two or more analyte molecules or particles occupy a volume encompassing what becomes a final electrosprayed droplet. This scenario would result in the observation of oligomers that originated from the droplet formation process.

The usual procedure in the use of a DMA is to charge neutralize the droplets with a bi-polar ion source (e.g Po-210), to yield a bipolar equilibrium charge distribution[16,17]. The neutralizer stops the fission process at an early stage leading to larger final droplet sizes. In such a situation, the charge residue model(CRM) is expected to hold and solvent evaporation could lead to unintentional analyte oligomers. Lenggoro *et al.*[18] and Pease *et al*[6]**.** have presented a method to provide an upper workable concentration to mitigate this problem. Kaufman *et al.*[1] have also described a simple criterion to determine whether there are intrinsic dimers in solution based on DMA size distributions. However, that criterion can not quantify the intrinsic aggregates in solution. The same evidence of unintentional analyte aggregation is also seen in ES without a neutralizer, using data found in the literature. While the final droplet size is much smaller because of a series of fissions, the net effect is the same.

This paper is focused on developing an experimentally verified theory that will enable one to distinguish ES induced aggregates from intrinsic aggregates, and without the need to model the details of the ES-Fission process, through a direct measure of the final droplet size distribution. We demonstrate our theory on experimental data found in the literature (ES-MS) and our own ES- DMA work. The approach is generic to any ES process and thus can be applied equally to either ion-mobility or mass spectrometry analysis.

2. Theory

2.1 Physical Aggregation (droplet induced aggregation) of identical particles

Because the spatial distribution of analytes in solution is statistical, our theoretical treatment was developed by probabilistic analysis. If a final droplet generated in ES is a random sample of the solution, and the particles in the solution are identical and independent, the probability of ***k*** particles in a given droplet obeys a Poisson distribution[1,19] and is given by

$$Q(k,\lambda) = \frac{e^{-\lambda}\lambda^{k}}{k!} \qquad (1)$$

where λ is the mean number of particles per droplet and is given by

$$\lambda = V_d C_p = \frac{1}{6}\pi D_d^{3} C_p$$

(2)

where V_d is the droplet volume, D_d is the droplet diameter and C_p is the number concentration of the particles in solution.

Lewis *et al.*[19] and Kaufman *et al.*[1] asserted that the probability to find a certain number of particles in a single droplet follows a Poisson distribution, but did not provide a justification. We use a statistical model to justify mathematically that particles indeed follow a Poisson distribution in solution. This model is discussed in greater detail in the supplementary section.

Consider a solution containing an analyte (particles). In the period of time that one unit volume of solution is sprayed, $1/V_d$ droplets are generated, and the total number of particles passing through the capillary and thus incorporated within the droplets is C_p. If we define one event as one particle being encapsulated in a droplet, and assign Δt as the average time to generate one droplet, then the rate of this event occurring is $R=C_p/(\Delta t*1/V_d) = V_dC_p/\Delta t$. The expected number of occurrences in this interval Δt is $\lambda = R\Delta t = V_dC_p$. The probability that there are exactly *k* occurrences in this interval is given by a Poisson distribution with parameter λ, $Q(k, \lambda)$, based on the definition of a Poisson distribution. Further justification on the use of a Poisson distribution is provided in supplemental information.

Assuming a droplet size distribution $f(D_d)$, the average value of parameter λ is given by

$$\overline{\lambda} = \sum_i f(D_{d,i})\lambda = C_p \sum_i \frac{1}{6}\pi D_{d,i}^{\ 3} f(D_{d,i}) = C_p \overline{V_d} \tag{3}$$

where $\overline{V_d} = \sum_i \frac{1}{6}\pi D_{d,i}^{\ 3} f(D_{d,i})$ is the average droplet volume. (4)

$$\sum_i f(D_{d,i}) = 1$$

The discussion about droplet size measurement is addressed in section 3.4.

Then the probability of droplet induced aggregation follows,

$$Q(k, \overline{\lambda}) = \frac{e^{-\overline{\lambda}}\overline{\lambda}^k}{k!} \tag{5}$$

where *k* is the order of aggregation.

If the solution contains only monomers, then based on Eqn. (5), the droplet induced dimer to monomer ratio is

$$\frac{Q(2, \overline{\lambda})}{Q(1, \overline{\lambda})} = \frac{\overline{\lambda}}{2} \tag{6}$$

In this scenario, there are no intrinsic dimers in solution. Therefore, the observed dimer to monomer ratio is the same as the induced ratio.

Equation 6 is useful because it provides a convenient criterion to determine if there are any intrinsic dimers in solution. Simply, if the observed dimers are higher than that computed by Eqn (6), we can ascribe the difference to intrinsic dimers in solution. This point has also been partially addressed by Kaufman *et al.*[1], but he assumed that all droplets were of the same size.

2.2 Quantitative determination of intrinsic aggregates in solution

The "dimer-to-monomer ratio" criterion, as demonstrated above, is valid if there are few to no dimers existing in the solution, but it fails where the intrinsic oligomers such as dimers, trimers etc. have a substantial contribution to the total particle concentration, as is common for solutions containing protein oligomers. In this section we present a strategy to quantify the aggregate ratio of intrinsic dimers to intrinsic monomers in solution for an arbitrary condition. This same strategy can also be expanded to quantify any higher-order aggregates. Before addressing the mathematics of the process, we consider the physical constructs of the problem.

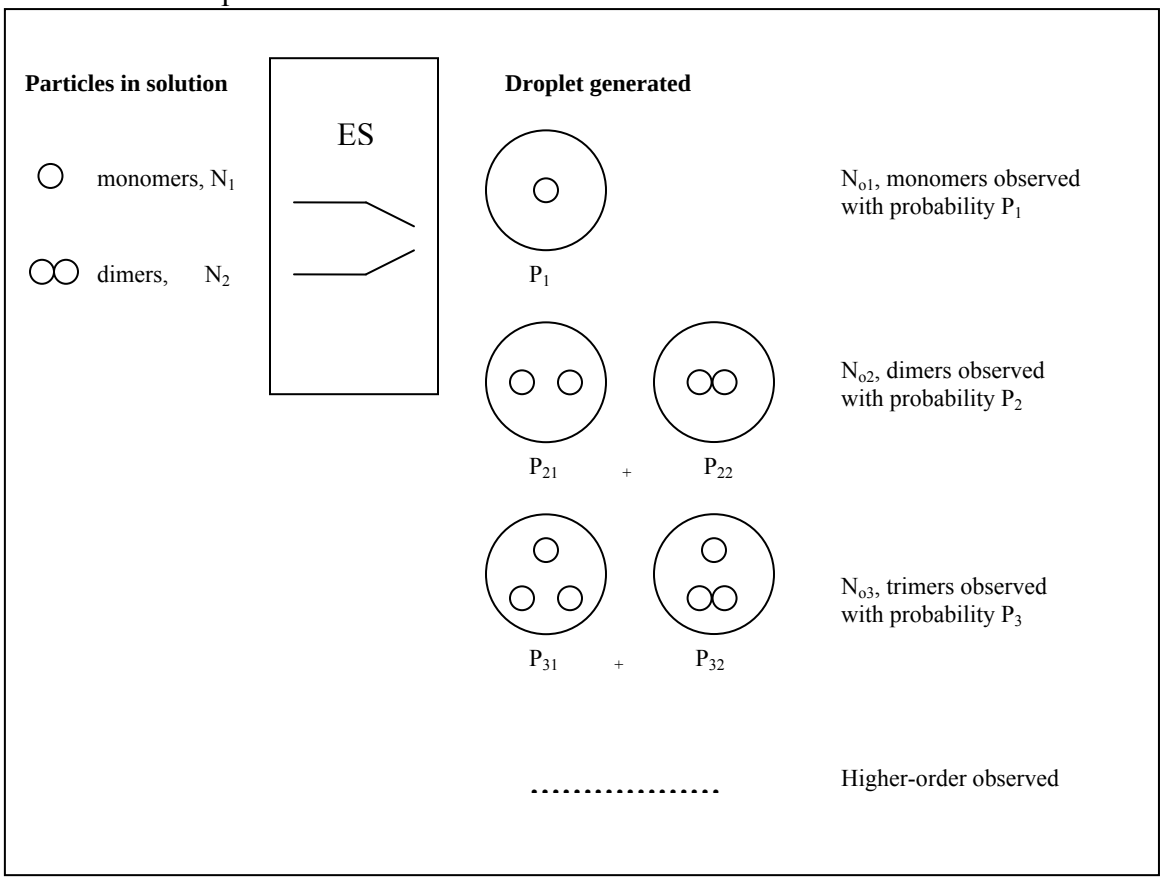

Figure 1. *Physical representation of the probability distribution of induced and intrinsic aggregate distributions from electrospray.*

A schematic description of how intrinsic and induced oligomers may be distributed within ES droplets is shown in Figure 1. Consider there are N_1 monomers and N_2 dimers in solution. Following ES, N_{o1} monomers, N_{o2} dimers, and N_{o3} trimers are observed with probabilities P_1, P_2 and P_3. There is only one possible condition for observation of monomers; that is, only one monomer in a single droplet generated by ES has a probability of P_1. For observed dimers, there are two possibilities. One is that two monomers are captured within a single droplet with probability P_{21}, creating an induced dimer, and the other possibility is that there is one intrinsic dimer in a single droplet with probability P_{22}. Similarly for trimers, there are two situations, three monomers captured into a droplet with probability P_{31} or one monomer and one dimer captured within the same droplet with probability P_{32}. With this construct we can obtain the following two relationships:

$$\frac{N_{o2}}{N_{o1}} = \frac{P_2}{P_1} = \frac{P_{21} + P_{22}}{P_1} \tag{7}$$

$$\frac{N_{o3}}{N_{o1}} = \frac{P_3}{P_1} = \frac{P_{31} + P_{32}}{P_1} \tag{8}$$

Assuming the spatial distribution of monomers is random, the number of monomers in a droplet should follow a Poisson distribution with parameter λ_1,

$$Q(k, \lambda_1) = \frac{e^{-\lambda_1} \lambda_1^{\,k}}{k!} \tag{9}$$

where $$\lambda_1 = V_d C_{p1} = \frac{1}{6} \pi D_d^{\,3} C_{p1} \tag{10}$$

C_{p1} the number concentration of monomers in solution
V_d the droplet volume
D_d the droplet diameter

The number of dimers in a droplet follows a Poisson distribution with parameter λ_2,

$$Q(k, \lambda_2) = \frac{e^{-\lambda_2} \lambda_2^{\,k}}{k!} \tag{11}$$

where $$\lambda_2 = V_d C_{p2} = \frac{1}{6} \pi D_d^{\,3} C_{p2} \tag{12}$$

C_{p2} the number concentration of dimers in solution

Assuming the two Poisson distributions are independent, so

$$P_1 = Q(1, \lambda_1) Q(0, \lambda_2) = e^{-(\lambda_1 + \lambda_2)} \lambda_1 \tag{13}$$

$$P_{21} = Q(2, \lambda_1) Q(0, \lambda_2) = e^{-(\lambda_1 + \lambda_2)} \frac{\lambda_1^{\,2}}{2}$$

(14)

$$P_{22} = Q(0,\lambda_1)Q(1,\lambda_2) = e^{-(\lambda_1+\lambda_2)}\lambda_2 \quad (15)$$

$$P_{31} = Q(3,\lambda_1)Q(0,\lambda_2) = e^{-(\lambda_1+\lambda_2)}\frac{\lambda_1^3}{6} \quad (16)$$

$$P_{32} = Q(1,\lambda_1)Q(1,\lambda_2) = e^{-(\lambda_1+\lambda_2)}\lambda_1\lambda_2 \quad (17)$$

.

Using relations (13), (14), (15), (16), (17), (7) and (8) we get

$$\frac{N_{o2}}{N_{o1}} = \frac{\lambda_1}{2} + \frac{\lambda_2}{\lambda_1} \quad (18)$$

$$\frac{N_{o3}}{N_{o1}} = \frac{\lambda_1^2}{6} + \lambda_2 \quad (19)$$

where

$$\lambda_1 = V_d C_{p1} \quad (10)$$

$$\lambda_2 = V_d C_{p2} \quad (12)$$

Eqns.(13) to (17) were obtained assuming that oligomers in ES process follow an independent joint Poisson distribution. An accurate form of (P1, P2) can be obtained using the methodology described in the statistic supplementary section. We use Eqns.(13) to (17) here for the calculations in this work.

Now, assuming a droplet size distribution f(D_d), using relations (18),(19),(10) and (12), and doing the averages to parameter λ_1 and λ_2, the ratios (N_{o2}/N_{o1} , N_{o3}/N_{o1}) are given by

$$\frac{N_{o2}}{N_{o1}} = \frac{\overline{V_d}C_{p1}}{2} + \frac{C_{p2}}{C_{p1}} \quad (20)$$

$$\frac{N_{o3}}{N_{o1}} = \frac{\overline{V_d}^2 C_{p1}^2}{6} + \overline{V_d}C_{p2} \quad (21)$$

where

$$\overline{V_d} = \sum_i f(D_{d,i})V_{d,i} = \sum_i f(D_{d,i})\frac{1}{6}\pi D_{d,i}^3 \quad (4)$$

$$\sum_i f(D_{d,i}) = 1$$

V_d the droplet volume

D_d the droplet diameter
$f(D_d)$ the droplet size distribution

The end result of this analysis shows that using experimental observation of the observed monomers, dimers and trimers (N_{o1}, N_{o2}, N_{o3}) one can use relations (20) and (21) to obtain the concentration of intrinsic monomers and dimers (C_{p1}, C_{p2}).

3. Materials and Methods

We demonstrate our model by examining gold nanoparticles (Au-NPs) with an ES-Neutralizer-DMA-CPC system described previously[20]. In order to show the efficacy of this technique, highly concentrated Au-NPs and large volume droplets in ES are needed. ES of highly concentrated Au-NPs is challenging because of the instability of the capillary that arises from the highly concentrated Au-NPs under low ionic strength and the presence of solution stabilizing citrate salts which can result in the formation of non-volatile particles that interfere with the DMA measurement[20]. The protocol for obtaining high concentrations of Au-NP is given below and large droplet sizes can be obtained by using low conductivity solutions along with large capillary diameters for the electrospray.

Finally we use Rituxan monoclonal antibody (Rmab) to show application of our approach to quantify protein aggregate distributions in solution.

3.1 Gold (Au) nanoparticle (NP) preparation

Commercially available citrate-stablized monodisperse Au colloids (10 nm, 5.7×10^{12} particles/mL**,** Ted Pella Inc.) were used. A 1.5 mL solution of the as-received Au colloids was centrifuged at 13,200 rpm for 45 minutes, and 1.46 mL -1.47 mL of the supernatant was removed and replaced with an equivalent volume of aqueous 2 mmol/L ammonium acetate solution at pH 10. This step was performed to remove most of the citrate stabilizer which would otherwise coat the Au-NPs upon ES. The pH of the ammonium acetate solution was adjusted by addition of ammonium hydroxide. The solution then was centrifuged at 13,200 rpm again for 15 minutes and 1.4 mL of supernatant was removed to obtain a highly concentrated Au-NP sample that was then electrosprayed into the DMA-CPC system. At these high concentrations, the oligomer peaks were not resolved (data not shown), and hence these samples were diluted 2×, 4×, and 8×, for the ES studies.

3.2 Rmab solution preparation

Formulated Rmab was purified using a Protein A affinity column. Purified Rmab was stored at -18 ºC in 25 mmol/L Tris buffer, pH 7.4, with 0.01% NaN_3 added as a preservative. Immediately prior to use in ES studies, the storage buffer was exchanged for 20 mmol/L ammonium acetate, pH 10 by washing all salts from Rmab using a

centrifugal filter device with a weight cutoff of 30 kDa. The concentration of Rmab in 20 mmol/L ammonium acetate was adjusted to 1 mg/mL as verified by measuring the maximum absorbance at 280 nm and using a molar absorptivity of 236,020 $(mol/L)^{-1}cm^{-1}$. Working solutions of concentrations 100 µg/mL, 50 µg/mL, 25 µg/mL, 10 µg/mL, and 5 µg/mL were made by dilution and used for ES studies.

3.3 Particle Measurements

Aerosolized droplets were generated using a 40 µm inner diameter capillary for Au-NP samples and a 25 µm inner diameter capillary for Rmab mounted in an Electrospray Aerosol Generator (Model 3480, TSI Inc.) and the liquid flow rates through the capillaries were 433 nL/min and 66 nL/min respectively[21]. The ES was operated with a carrier gas of 1 L/min purified air and 0.2 L/min carbon dioxide. The aerosolized droplets were passed through a neutralizer and entered a Differential Mobility Analyzer (Model 3485 Nano DMA column, TSI Inc.) for particle size measurement, and counted with an Ultrafine Condensation Particle Counter (Model 3025A TSI Inc.) More details on the measurement method can be found in Tsai *et al.*[20] .

3.4 Droplet size Measurements

Use of relations (3) or (4) requires knowledge of the droplet size. Droplet size was determined by electrospraying a known concentration of sucrose solution and measuring the resultant dry particle size. The sucrose solution (1.26 % v/v) was prepared and diluted into 20 mmol/L ammonium acetate buffer, pH 10, giving a final concentration of 0.063% v/v. The ES droplet size of this solution was evaluated by[17]

$$D_d = \frac{1}{C_s^{1/3}} D_s \tag{22}$$

where D_d is the droplet diameter, D_s is the sucrose particle diameter after drying, and C_s is the sucrose volume/volume concentration.

Note, an alternative approach discussed in the next section that involves measurement of a series dilutions of the original analyte mitigates the need to know the drop size distribution

4. Results and Discussion

4.1 Intrinsic Dimer determination for Au-NP samples

In this section, we discuss the implementation of an experimental strategy, based on the relationships derived in the previous section, in which we determine intrinsic aggregate concentration.

Firstly, the sucrose size distributions in the 20 mmol/L Ammonium Acetate buffer at pH 10 were obtained that provide us with the droplet size distributions for Au-NPs using Eqn. (22),

The ratio of intrinsic dimer to monomer of Au-NPs were then obtained by a series of measurements at various dilutions.

Based on Eqn. (20), after a 2× dilution, an additional relationship can be obtained,

$$\frac{N_{o2,2x}}{N_{o1,2x}} = \frac{\overline{V_d} C_{p1}/2}{2} + \frac{C_{p2}/2}{C_{p1}/2} = \frac{\overline{V_d} C_{p1}}{4} + \frac{C_{p2}}{C_{p1}} \tag{23}$$

where $N_{o1,2x}$ is the observed number of monomers after 2× dilution and $N_{o2,2x}$ is the observed number of dimers after 2× dilution.

Combining (20) and (23), the ratio of intrinsic dimer to monomer of Au-NPs is

$$\frac{C_{p2}}{C_{p1}} = 2\frac{N_{o2,2x}}{N_{o1,2x}} - \frac{N_{o2}}{N_{o1}} \tag{24}$$

Figure 2 shows the observed size distribution at 2×, 4× and 8× dilutions for 10 nm Au-NPs (sample #1). The DMA voltage was scanned to detect particles up to 20 nm to enable measurement of trimers that could be observed for the 2× dilution, but not for more dilute samples.

Table 1 shows the ratios of dimer to monomer measured with ES-DMA at 2×, 4× and 8× dilutions of Au-NPs (sample #1 to sample #4). A large proportion of oligomers are observed in these measurements. Using the theory described above we now determine the true oligomer concentration.

For each sample, the ratio of intrinsic dimer to monomer is calculated based on Eqn. (24), using the ratio of 2× and 4× dilution and 4× and 8× dilution. Given the instability of the ES cone-jet at low ionic strength and the propensity of the highly concentrated Au-NPs to aggregate, the intrinsic ratios calculated using 2× and 4× dilution and using 4× and 8× dilution are mostly consistent. We note that with the dilution approach, it is not necessary to know the droplet size.

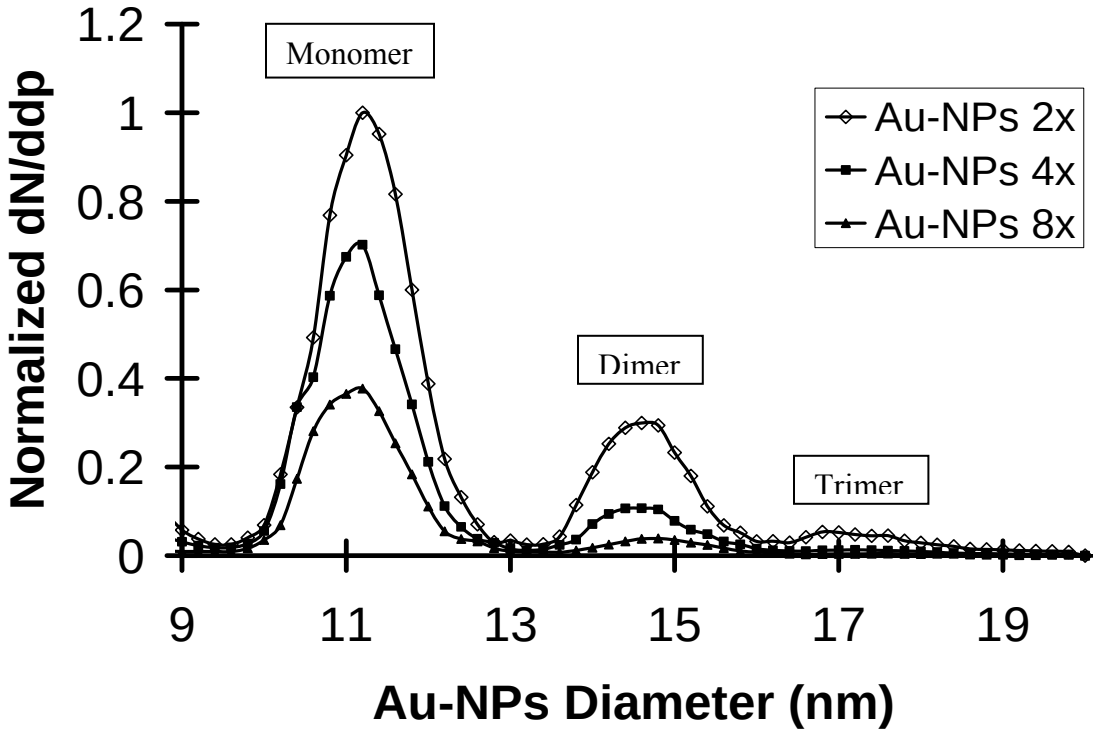

Figure 2. *ES-DMA size distributions of 10 nm Au-NPs, sample #1. The rhombus, square and triangle data markers are those of 2-times, 4-times and 8-times dilutions of the original sample, respectively. Each of the discernable oligomer peaks are labeled.*

Table 1. *Ratios of observed dimers to monomers from DMA measurement, and the ratios of intrinsic dimers to monomers calculated based on Eqn. (24) for 10nm Au-NPs.*

	ES-DMA observed dimer to monomer ratio			True dimer to monomer ratio (i.e. after droplet induced effects removed)	
	2x	4x	8x	based on 2x and 4x	Based on 4x and 8x
Sample #1	31.3%	17.3%	11.5%	3.3%	5.7%
Sample #2	33.2%	18.1%	12.3%	3.0%	6.5%
Sample #3	36.3%	19.5%	11.1%	2.7%	2.7%
Sample #4	35.7%	19.4%	12.1%	3.1%	4.8%

4.2 Evidence of droplet induced aggregation

To illustrate the magnitude of the problem and the errors that can occur if the droplet induced effects are not accounted for, we consider two examples. The first is an ES-MS (without a neutralizer) study by Nettleton *et al.*[10] to characterize the oligomers of insulin and the second where Rmab samples were measured by our ES-Neutralizer-DMA-CPC system.

Nettleton *et al.*[10] plotted the fraction of dimer observed by MS against the insulin concentration from 2 μmol/L to 200 μmol/L at pH 3.3 and 22°C (Figure 3, rhombus). The fraction of dimer was defined as the ratio of summation of the peaks assigned to the dimer to the total signal intensity. In this insulin concentration range only monomer and dimer peaks were observed by MS, so the fraction of dimer is equal to the number of observed dimers divided by the total number of observed dimers and monomers. Based on droplet induced aggregation of identical particles following Eqn. (5), the fraction of induced dimer is

$$\frac{N_{o2}}{N_{o1}+N_{o2}} = \frac{P(2,\bar{\lambda})}{P(1,\bar{\lambda})+P(2,\bar{\lambda})} = \frac{\bar{\lambda}}{2+\bar{\lambda}} = \frac{C_p\bar{V}_d}{2+C_p\bar{V}_d} \tag{25}$$

where $\bar{V}_d$ is the average droplet volume, and C_p is the insulin number concentration.

Since we do not know the droplet sizes used by Nettleton *et al.*[10], we estimate the droplet size by using the protein concentration and the ratio of dimer to total oligomer (Eqn. 25). The fourth point in Nettleton's plot is then given by $\log_{10}[Cp]= -4.3$ and the fraction of dimer = 0.6. This value is used to estimate the average droplet volume as ca. $9.943\times10^{-23}m^3$.

We then use this average droplet volume to calculate the fraction of dimer at other concentrations in Nettleton's plot based on Eqn. (25) and obtain the curve in Figure 3 (line with filled squares). The curve deduced from the droplet induced model essentially superimposes on Nettleton's data. The fact that the two curves track each other so closely is, we believe, clear evidence that the Nettleton data do not represent oligomers in solution but instead are an artifact of droplet induced aggregation occurring during the ES process.

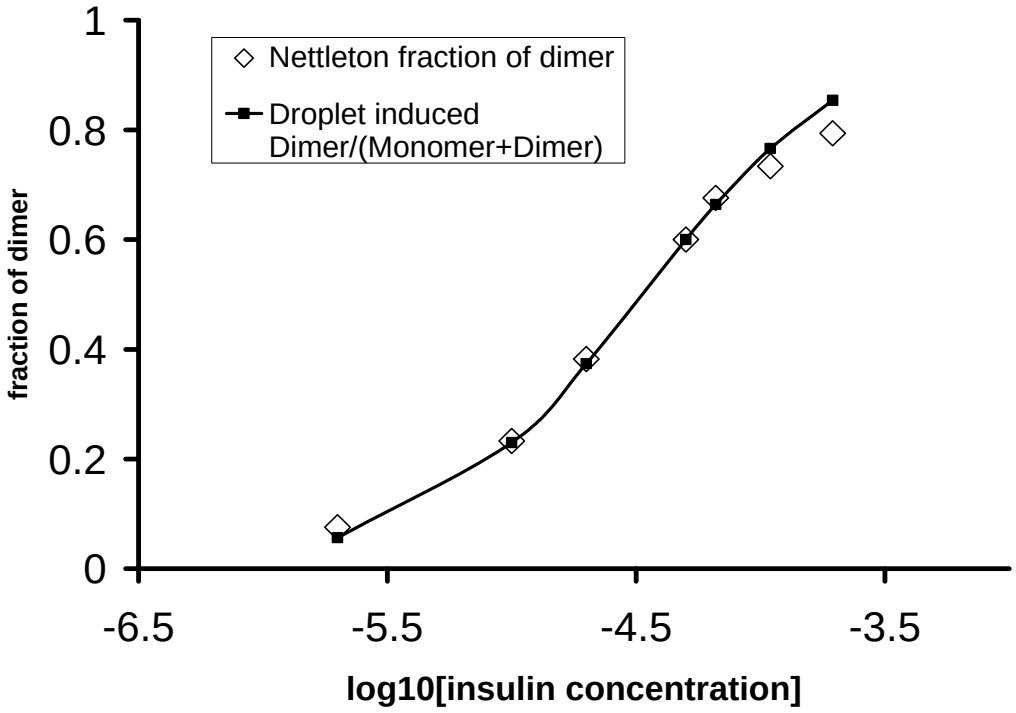

Figure 3. *The fraction of insulin dimer vs. insulin total in the concentration range of 2 μmol/L to 200 μmol/L at pH 3.3 and 22°C (rhombus) as measured by Nettleton et al.[10] using Nano-ES/MS (line with open diamonds). The ratio of dimer / (monomer + dimer) calculated by Eqn. (25) using the droplet induced dimer for the concentration range of 2 μmol/L to 200 μmol/L (line with filled squares).*

The same characteristics of droplet induced aggregation are also observed in our ES-DMA measurements. Figure 4 shows the droplet size distributions at pH 10 in 20 mmol/L ammonium acetate buffer of Rituxan at concentrations of 5 μg/mL, 10 μg/mL, 25 μg/mL, 50 μg/mL, and 100 μg/mL. Based on the distribution in Figure 4 and Eqn.(4), the average droplet volume was calculated to be $1.321*10^{-21}m^3$. The average droplet size is 131 nm which is in reasonable agreement with previous results[6,18,22]. According to Pease *et al.*[6] the corresponding "cut-off" concentration at which observed aggregates are intrinsic to the sample is 212 μg/mL.

The ratios of the number of observed dimer to the total number of observed dimer and monomer against the Rituxan concentration at 5 μg/mL, 10 μg/mL, 25 μg/mL, 50 μg/mL, and 100 μg/mL are plotted in Figure 5 (rhombus). Based on Eqn. (25), we also calculate the ratios of the number of dimers to the total number of dimer and monomer at the same concentrations and obtain a second curve in Figure 5 (line with filled square). The curve deduced from the droplet induced model lies slightly below the data points indicating that most dimers observed in Figure 5 by ES-DMA are droplet induced and that the "cut-off" criterion as used by Lenggoro *et al*[18]. and Pease *et al.*[6] is insufficient in eliminating droplet induced aggregation effects. Hence we conclude that induced aggregation is a problem at all concentrations and that the approach described above should be used to determine the extent of physical aggregation. To a first approximation, the difference

between the experimental data and the induced dimer curve can provide the true dimer concentration. A more rigorous approach is to include the effect of intrinsic dimer present in the sample. When intrinsic dimer is present, the concentration of monomer is lower, and thus, the induced dimer fraction will also be lower. This issue could be solved using an iterative procedure; however, we described a simpler approach below in the next section.

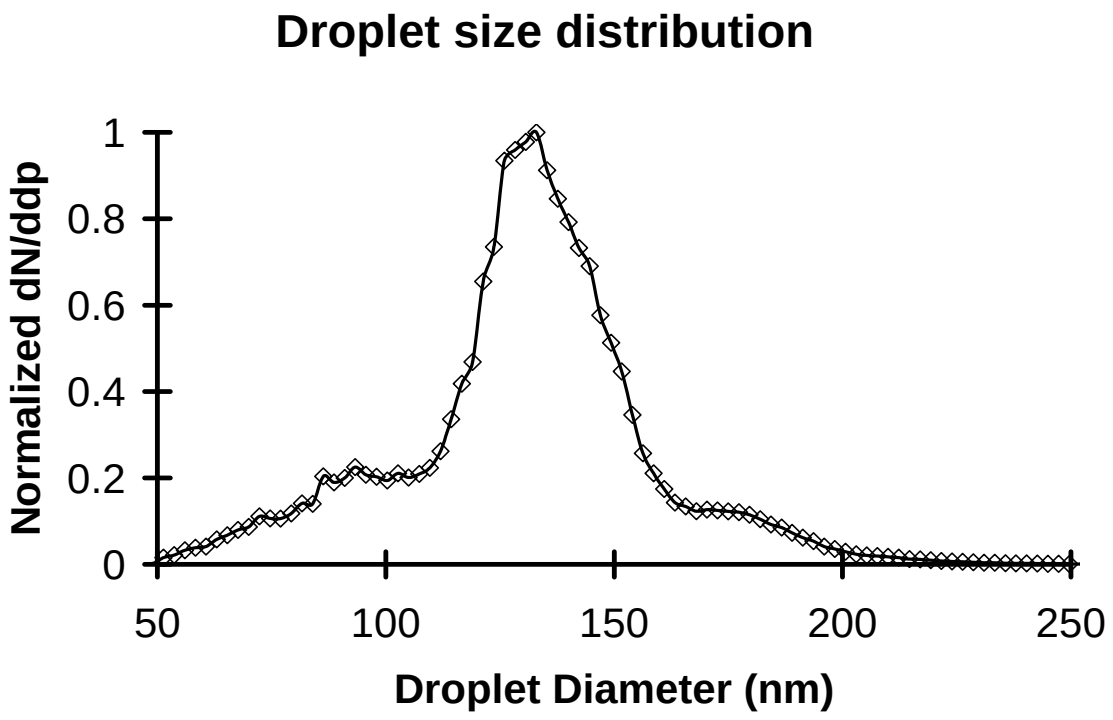

Figure 4. *ES droplet size distribution at pH 10 in 20 mmol/L ammonium acetate buffer.*

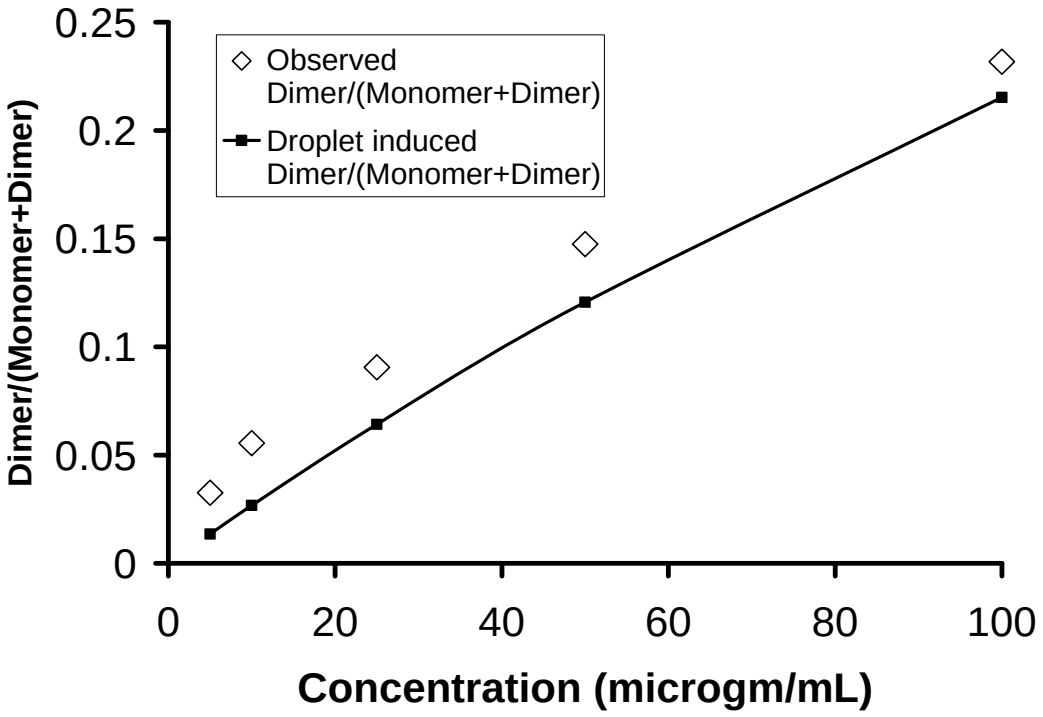

Figure 5. *The ratios of dimer to the total number of dimer and monomers observed by ES-DMA as a function of Rituxan concentration at 5 µg/mL, 10 µg/mL, 25 µg/mL, 50 µg/mL, and 100 µg/mL (rhombus). Ratios from droplet induced dimers (line with filled square) at the same concentrations calculated based on Eqn. (25).*

These two examples clearly illustrate that care must be taken in interpreting results of oligomer distributions measured from an ES source regardless of the analytical tool used to detect the particles. This point is particularly relevant for ES sources for MS characterization where multiply charged analytes are characterized, so that distinguishing a doubly charged dimer from a singly charged monomer must be accounted for.

4.3 Intrinsic Dimer determination: Oligomerization of Rmab

In this section we show a strategy to determine the concentration of intrinsic aggregates.

If we assume that only monomers and dimers are in solution and no higher aggregates, and that the total concentration C_p is known, an additional relationship can be obtained,

$$C_p = C_{p1} + 2C_{p2} \tag{26}$$

The ratio of intrinsic dimer to monomer of Rmab, C_{p2}/C_{p1}, can be obtained from (20) and (26).

Table 2 shows the ratios of observed dimers to monomers for Rituxan measured in ES-DMA experiments at concentrations of 5 μg/mL, 10 μg/mL, 25 μg/mL, 50 μg/mL, and 100 μg/mL, the intrinsic ratios at the same concentrations calculated based on Eqns. (20) and (26).

Table 2. *The ratios of observed dimers to monomers from DMA measurement, the ratios of intrinsic dimers to monomers calculated based on Eqn. (20,26) and the ratio of dimers to monomers measured by Analytical Ultracentrifuge for Rmab*

	ES-DMA observed dimer to monomer ratio	Intrinsic dimer to monomer ratio after correction for drop induced dimers.	Analytical Ultracentrifuge measured dimer to momomer ratio
5 μg/mL	3.4%	2.1%	NA
10 μg/mL	5.9%	3.3%	NA
25 μg/mL	10.0%	3.6%	NA
50 μg/mL	17.3%	4.8%	NA
100 μg/mL	30.2%	5.4%	4.7%

The results in Table 2 demonstrate that the actual dimer concentration in solution can be considerably smaller than that measured using an ES source, particularly at high concentration. For example at 100 μg/mL the observed dimer-to-monomer was ~ 30%, while after correction, the intrinsic ratio is 5.4%. At this high concentration we were also able to compare with Analytical Ultracentrifuge[23,24] measurements directly on the solution, under the same conditions, which showed very good agreement with our corrected value.

Conclusions

ES sampling is widely used to introduce non-volatile material into the gas phase for characterization by MS or DMA. In using an ES sampling process for characterizing protein or nanoparticle aggregation, one must carefully evaluate if aggregates observed are intrinsic to the solution or induced by the ES process. We have developed a statistical model to calculate the intrinsic oligomer ratios in solution from the experimentally determined distributions by considering the droplet size distribution and physical induced aggregation in electrosprays. Using this approach, we show that that the extent of droplet induced aggregation can be severe. We demonstrate that droplet induced aggregation can bias data obtained by either ES-MS or ES-DMA and that data obtained by these methods need to be carefully scrutinized to avoid erroneous interpretation. Based on our experimentally validated model, a quantitative distribution of intrinsic particle aggregation in electrospray can be obtained.

Acknowledgment:

The authors thank Dr. James Falabella for providing us data from his Analytical Centrifuge measurements of Rmab. Commercial equipment, instruments, or materials identified in this report does not imply recommendation or endorsement by the University of Maryland or the National Institute of Standards and Technology.

Supplemental Information

This Appendix provides a justification for the use of a Poisson distribution.
A statistic model is developed to calculate the induced aggregates formed in the electrospray droplets as they dry.

In this paper, we have only developed a Monomer-Dimer model,however more complicated models can be developed using the same strategy

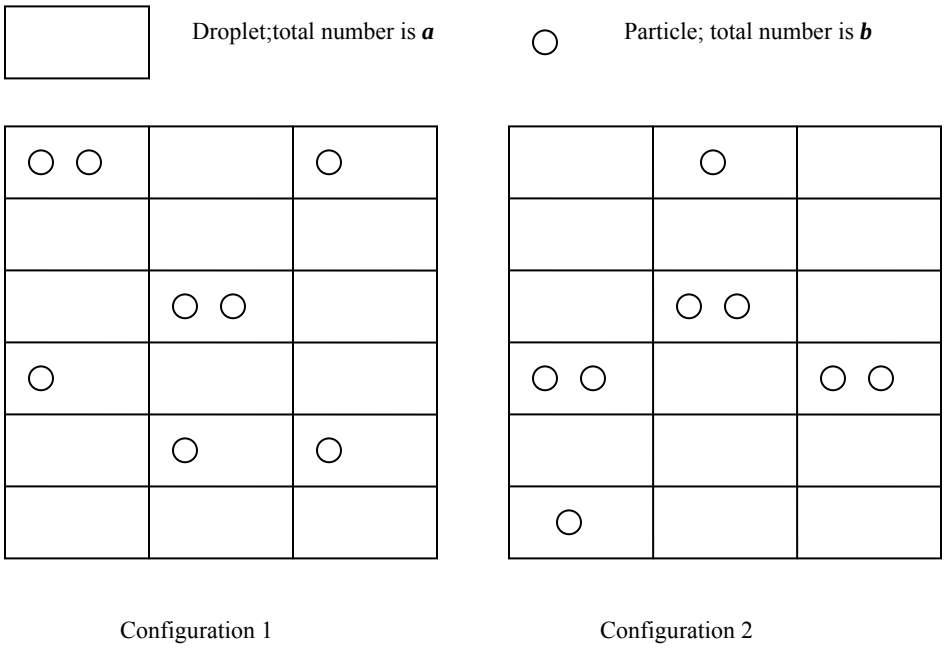

Figure A.1. ***b*** particles randomly distributed in ***a*** droplets

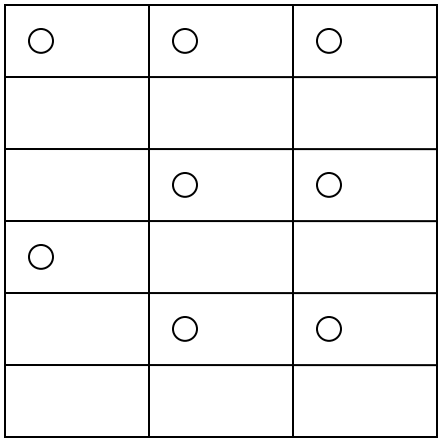

Figure A.2. No dimers.

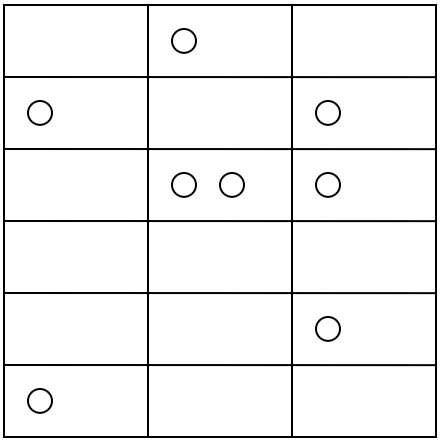

Figure A.3. One dimer and remainder are monomers

Monomer-Dimer model.

In Figure A.1 we show that assuming only monomer in solution and there are ***b*** particles randomly distributed in ***a*** droplets, that there are many possible configurations.

There are 3 assumptions for this model:

1. The maximum number of particles in one droplet is 2.
2. The probability of each configuration is equal.
3. Droplets are distinguishable; particles are distinguishable.

Assuming ***b*** is an even number, there are 1+***b***/2 cases for this model.

Case 0. No dimers, (**Figure A.2)**. The number of configurations in this case is,

$$P_{2,0}(a,b) = P_1(a,b) = C(a,b)b! \tag{A.1}$$

Where C(***a***,***b***) is the binomial coefficient, number of ***b***-combinations (each of size ***b***) from a set with ***a*** elements (size ***a***).

Case 1. One dimer and ***b-2*** are monomers, showed in **Figure A.3**. The number of configurations in this case is,

$$P_{2,1}(a,b) = C(a,1)C(b,2)P_1(a-1,b-2) \tag{A.2}$$

……

Case ***i***. There are ***i*** dimers and ***b-2i*** monomers. The number of configurations in this case is,

$$P_{2,i}(a,b) = C(a,i)C(b,2i)\frac{(2i)!}{(2!)^i}P_1(a-i,b-2i) \tag{A.3}$$

……

Case ***b***/2. All are dimers. The number of configurations in this case is,

$$P_{2,b/2}(a,b) = C(a,b/2)\frac{(b)!}{(2!)^{b/2}}P_1(a-b/2,0) \quad \text{(A.4)}$$

In Case ***i***, the number of monomers is (***b-2i***)$P_{2,i}$(***a***,***b***), and the number of dimers is ***i***$P_{2,i}$(***a***,***b***). So the total number of monomers in all cases is,

$$N_{2,m}(a,b) = \sum_{i=0}^{b/2}(b-2i)P_{2,i}(a,b) \quad \text{(A.5)}$$

and the total number of dimers in all cases is,

$$N_{2,d}(a,b) = \sum_{i=0}^{b/2} iP_{2,i}(a,b) \quad \text{(A.6)}$$

Substituting Eqs.(A.3) for $P_{2,i}$(***a***,***b***) in Eqs.(A.5), the following result is obtained:

$$N_{2,m}(a,b) = \sum_{i=0}^{b/2} C(a,i)C(b,2i)\frac{(2i)!}{(2!)^i}(b-2i)P_1(a-i,b-2i) \quad \text{(A.7)}$$

Similarly, substituting Eqs.(A.3) for $P_{2,i}$(***a***,***b***) in Eqs.(A.6), the total number of dimers can be expressed as,

$$N_{2,d}(a,b) = \sum_{i=0}^{b/2} C(a,i)C(b,2i)\frac{(2i)!}{(2!)^i} iP_1(a-i,b-2i) \quad \text{(A.8)}$$

The ratio of the number of dimers to the number of monomers based on this model is,

$$R_{2,d}(a,b) = N_{2,d}(a,b)/N_{2,m}(a,b) \quad \text{(A.9)}$$

Because in a specific experiment, ***a*** and ***b*** can be chosen arbitrarily, but the mean number of particles per droplet, $\lambda = \boldsymbol{b}/\boldsymbol{a} = V_dC_p$ is a characteristic value for that experiment, where V_d is the droplet volume and C_p is the number concentration of the monomer particles in solution. An asymptotic relationship between $R_{2,d}$ and λ when ***a*** is large; ***a=15000*** (λ =***b/a*** =0.05, 0.1, 0.15, 0.2, 0.25, 0.3) is

$$R_{2,d}(a,b) = N_{2,d}(a,b)/N_{2,m}(a,b) = 0.5215\lambda - 0.0018 \quad \text{(A.10)}$$

The relationship derived in Equation A.10 gives an accurate relationship for the ratio of dimers to monomers (for no higher oligomers), and is very close to what a Poisson distribution gives i.e.

$$R_{2,d} = 0.5\lambda \quad \text{(A.11)}$$

We therefore employ a Poisson distribution approximation for the derivation of the relationships derived in the body of the manuscript.

Reference:

(1) Kaufman, S. L.; Skogen, J. W.; Dorman, F. D.; Zarrin, F. *Anal. Chem.* **1996**, *68*, 1895

(2) Bacher, G.; Szymanski, W. W.; Kaufman, S. L.; Zo¨llner, P.; Blaas, D.; Allmaier, G. n. *J. Mass Spectrom.* **2001**, *36*, 1038

(3) Kim, S. H.; Zachariah, M. R. *Nanotechnology* **2005**, *16*, 2149

(4) Kim, S. H.; Zachariah, M. R. *J. Phys. Chem. B* **2006**, *110*, 4555

(5) Kim, S. H.; Zachariah, M. R. *Mater. Lett.* **2007**, *61*, 2079

(6) III, L. F. P.; Elliott, J. T.; Tsai, D.-H.; Zachariah, M. R.; Tarlov, M. J. *Biotechnol. Bioeng.* **2008**, *101*, 1214

(7) Light-Wahl, K. J.; Winger, B. E.; Smith, R. D. *J. Am. Chem. Soc.* **1993**, *115*, 5869

(8) Light-Wahl, K. J.; Schwartz, B. L.; Smith, R. D. *J. Am. Chem. Soc.* **1994**, *116*, 5271

(9) Ayed, A.; Krutchinsky, A. N.; Ens, W.; Standing, K. G.; Duckworth, H. W. *Rapid Commun. Mass Spectrom.* **1998**, *12*, 339

(10) Nettleton, E. J.; Paula Tito, M. S.; Bouchard, M.; Dobson, C. M.; Robinson, C. V. *Biophys. J.* **2000**, *79*, 1053

(11) Kebarle, P.; Tang, L. *Anal. Chem.* **1993**, *65*, 972

(12) Gaskell, S. J. *J. Mass Spectrom.* **1997**, *32*, 677

(13) Dole, M.; Mack, L. L.; Hines, R. L. *J. Chem. Phys.* **1968**, *49*, 2240.

(14) Iribarne, J. V.; Thomson, B. A. *J. Chem. Phys.* **1976**, *64*, 2287.

(15) Kebarle, P. *J. Mass Spectrom.* **2000**, *35*, 804.

(16) Wiedensohler, A. *J. Aerosol Sci.* **1988**, *19*, 387.

(17) Chen, D.-R.; Pui, D. Y. H.; Kaufman, S. L. *J. Aerosol Sci.* **1995**, *6*, 963

(18) Lenggoro, I. W.; Xia, B.; Okuyama, K. *Langmuir* **2002**, *18*, 4584

(19) Lewis, K. C.; Dohmeier, D. M.; Jorgenson, J. W. *Anal. Chem.* **1994**, *66*, 2285

(20) Tsai, D.-H.; Zangmeister, R. A.; III, L. F. P.; Tarlov, M. J.; Zachariah, M. R. *Langmuir* **2008**, *24*, 8483

(21) *TSI Model 3480 Electrospray Aerosol Generator Menu TSI inc.*

(22) Kaufman, S. L. *Anal. Chim. Acta* **2000**, *406*, 3.

(23) Ebel, C. *Prog. Colloid Polym. Sci.* **2004**, *127*, 73.

(24) Howlett, G. J.; Minton, A. P.; Rivas, G. *Curr. Opin. Chem. Biol.* **2006**, *10*, 430.